ANTIOXIDANTS & REDOX SIGNALING
Volume 16, Number 4, 2012

DOI: 10.1089/ars.2011.4232

ORIGINAL RESEARCH COMMUNICATION

Curcumin Heals Indomethacin-Induced Gastric Ulceration by Stimulation of Angiogenesis and Restitution of Collagen Fibers *via* VEGF and MMP-2 Mediated Signaling

Anamika Vivek Sharma,[1,*] Krishnendu Ganguly,[1,*] Sumit Paul,[1] Nilanjana Maulik,[2] and Snehasikta Swarnakar[1]

Abstract

Aim: We examined the molecular mechanism of curcumin in a preventive and therapeutic model of indomethacin-induced gastric ulceration with regard to angiogenic processes. ***Results:*** Disrupted blood vessels, reduced collagen matrices, and significant (60%) injury to mucosal cells were observed during ulceration. In addition, ulcerated tissues exhibited decreased matrix metalloproteinase (MMP)-2 and vascular endothelial growth factor (VEGF) expression in blood vessels. Interestingly, curcumin blocked ulceration by induction of collagenization and angiogenesis in gastric tissues *via* upregulation of MMP-2, membrane type (MT) 1-MMP, VEGF, and transforming growth factor (TGF)-β at protein and messenger ribonucleic acid (mRNA) levels. To examine the angiogenic properties of curcumin, we employed a chorioallantoic membrane model and Matrigel assay. During healing, curcumin promoted collagenization and angiogenesis as well as enhanced MMP-2 activity *via* positive MT1-MMP regulation and negative tissue inhibitor of metalloproteinase-2 regulation. ***Innovation:*** Our study demonstrates that curcumin-mediated healing is associated with increased MMP-2, TGF-β, and VEGF expression and that it plays a pivotal role as an angiogenic modulator by stimulating vascular sprout formation and collagen fiber restoration in ulcerated tissues. ***Conclusion:*** We conclude that curcumin remodels gastric tissues by restoring the collagen architecture and accelerating angiogenesis. *Antioxid. Redox Signal*. 16, 351–362.

Introduction

Gastric ulcer healing is a complex process involving cellular proliferation, angiogenesis, and matrix remodeling, all of which ultimately lead to the restoration of tissue structure. Although gastric ulcer healing requires angiogenesis, few studies have reported the efficacy of angiogenic agents in promoting gastric ulcer healing (1, 10, 29, 30). During gastric ulcer healing, endothelial cells, under the effect of vascular endothelial growth factor (VEGF), proliferate to form microvessels and a capillary network in tissues (20). Transforming growth factor (TGF)-β accelerates angiogenesis by inducing matrix metalloproteinase (MMP) expression. MMPs degrade the basement membrane, extracellular matrix (ECM), and other ECM components during gastric ulcer formation (4, 6, 15, 18, 22, 25, 28, 31, 34). However, MMPs pro-

Innovation

This study is the first to demonstrate that curcumin possesses both angiogenic and anti-angiogenic properties, depending on the dosage used for a particular therapy. Curcumin is a well-known anti-angiogenic agent (2, 9); however, here we report that, at very low doses, curcumin stimulates healing both *in vitro* and *in vivo* by inducing vascular sprout formation and restoring collagen fibers in ulcerated tissues. These results strongly suggest that curcumin has both anti-angiogenic and angiogenic activity. Thus, curcumin could be a superior natural product and could be used (at judicious doses) for inducing or preventing angiogenesis, depending on the medical context.

[1]Department of Physiology, Drug Development Diagnostics and Biotechnology Division, Indian Institute of Chemical Biology, Kolkata, India.
[2]Department of Surgery, Molecular Cardiology and Angiogenesis Laboratory, University of Connecticut School of Medicine, Farmington, Connecticut.
*These authors contributed equally to this work.

mote wound healing by facilitating the migration of different cell types during neovascularization and collagenization (25). The active forms of ECM-bound proangiogenic factors, such as VEGF and TGF-β, are also cleaved by MMPs, which promote signaling associated with endothelial cell proliferation and angiogenesis during ulcer healing (1, 23, 25, 27, 29, 30).

Upon exposure to ulcerogenic agents, such as indomethacin, gastric tissues show characteristic changes leading to gastric injury (5, 28). The action of curcumin, an antioxidant from turmeric, has been extensively studied over the past few years, however, its mechanism of action in gastric ulcer healing remains unknown. Our previous studies have demonstrated that curcumin offers gastroprotection through regulation of MMP-9 and MMP-2 by alleviating inflammatory cytokines and redox-dependent signaling (14, 28). However, no study has been conducted to date to elucidate its angiogenic potential during gastric ulcer healing; however, some studies have shown that this elucidation is possible. For example, some Chinese herbs possess strong angiogenic activity, as has been shown by chick chorioallantoic membrane (CAM) and in cultured bovine aortic endothelial cells (33). In addition, the *Centella asiatica* plant extract has exhibited angiogenic activity during wound healing (26). A combination of antioxidants (proanthocyanidin and resveratrol) from grapeseed has also been shown to increase VEGF expression and angiogenesis (13). Furthermore, we recently reported that melatonin, a pineal hormone, promotes MMP-2-mediated angiogenesis during healing of indomethacin-induced gastric ulceration (6).

Here we report the novel functions of curcumin, namely, the promotion of neovessel formation and inhibition of collagenolysis during gastroprotection and healing of gastric ulcers. Increased angiogeneis is associated with MMP-2, MT 1-MMP, VEGF, and TGF-β induction, and inhibition of tissue inhibitor of metalloproteinase (TIMP)-2, all of which contribute to protection against ulcers associated with curcumin. Experiments performed using a CAM model and Matrigel assay suggest that low curcumin doses promote, whereas high doses prevent, angiogenesis. Similarly, curcumin promotes healing by enhancing TGF-β, VEGF, and MMP-2 expression and thereby restores the normal architecture of disrupted blood vessels. Our study is the first to demonstrate that curcumin induces angiogenesis *via* MMP-2 and VEGF overexpression, protecting against and healing gastric ulcers.

Results

Curcumin restores damaged blood vessels of ulcerated gastric tissues and induces MMP-2 and VEGF expression in rats

Our previous studies have demonstrated that curcumin prevents gastric epithelial cell damage due to indomethacin- and *Helicobactor pylori*-induced gastropathy because of its anti-oxidant and anti-inflammatory effects (14, 29). However, no study has examined the ECM structure and associated vasculature of gastric tissues. Therefore, in this study, we examined curcumin's effect at both the histological and molecular levels to gain deeper insight into its mechanism of action. Histological analysis showed that indomethacin caused denudation of the gastric mucosa and disrupted blood vessels in the submucosa (Fig. 1B), whereas curcumin pretreatment augmented the reappearance of intact blood vessels and a mucosal layer similar to that of the control tissues (Fig. 1A and C). In addition, indomethacin induced thrombosis and disruption of blood vessels (Fig. 1E), whereas curcumin pretreatment restored blood vessels to an intact status (like the control tissues) and restructured the lumen of the submucosa (Fig. 1D and F). Silver-stained control tissues showed intact tunica intima, media, and adventitia layers surrounded by an organized collagen matrix, possibly type III collagen, in blood vessels (Fig. 1G). Indomethacin treatment caused the merging of all endothelial layers with the surrounding connective tissue, where sparse and loose collagen bundles were observed around dilated and thrombosed blood vessels (Fig. 1H). However, curcumin pretreatment induced the reappearance of all the endothelial layers, along with the development of an organized collagen matrix (Fig. 1I). Various findings have shown that VEGF-mediated MMP-2 signaling is essential for gastroprotection (6, 25, 30). Therefore, we examined VEGF and MMP-2 localization in gastric tissues using immunofluorescence (Fig. 1M–R). The control gastric tissues exhibited VEGF expression in endothelial cells, indicating a well-nourished vasculature (Fig. 1M). However, in curcumin-pretreated tissues, VEGF overexpression was observed predominantly in the endothelial cells (Fig. 1O). VEGF localization (Fig. 1N) was reduced in the damaged blood vessels of ulcerated tissues. Similarly, decreased MMP-2 expression was restricted to the damaged blood vessels of ulcerated tissues (Fig. 1Q), whereas its overexpression was localized to a compartment of endothelial cells in curcumin-pretreated tissues (Fig. 1R). Phase contrast (Fig.1J–L) and fluorescence microscopy analyses revealed that curcumin-pretreated tissues exhibit a higher number of VEGF- and MMP-2-positive endothelial cells than ulcerated tissues. This finding suggests that curcumin pretreatment induced VEGF and MMP-2 overexpression and promoted clustering of endothelial cells within the gastric vasculature.

Curcumin blocks collagenolysis, preventing gastric ulceration

To investigate the role of curcumin in ECM maintenance *via* collagenization, we immunostained all the experimental tissues with Van Gieson stain. The Van Gieson-stained slides showed that collagen fibers were orderly and abundantly arranged in a systematic pattern in both the lamina propria and submucosa of the gastric tissues of control rats (Fig. 2A, a and d). Indomethacin treatment resulted in a sparse, thin, loose, and disordered collagen matrix (Fig. 2A, b and e), whereas curcumin pretreatment resulted in dense, organized collagen fibers, indicating that curcumin exerts its protective effect through collagenization (Fig. 2A, c and f). To quantify the collagen content in the different gastric tissues, hydroxyproline levels were assayed. The collagen content in indomethacin-treated tissues decreased approximately 1.5-fold compared to that in control tissues. Curcumin rescued the tissues by ameliorating the changes in hydroxyproline levels, indicating that it blocks collagen degradation during healing (Fig. 2B). Thus, it is conceivable that ulceration causes complete disorganization of the mucosal and submucosal ECM, whereas curcumin restores the proper homeostasis of ECM by increased deposition of collagen fibers in an orderly manner, providing gastroprotection.

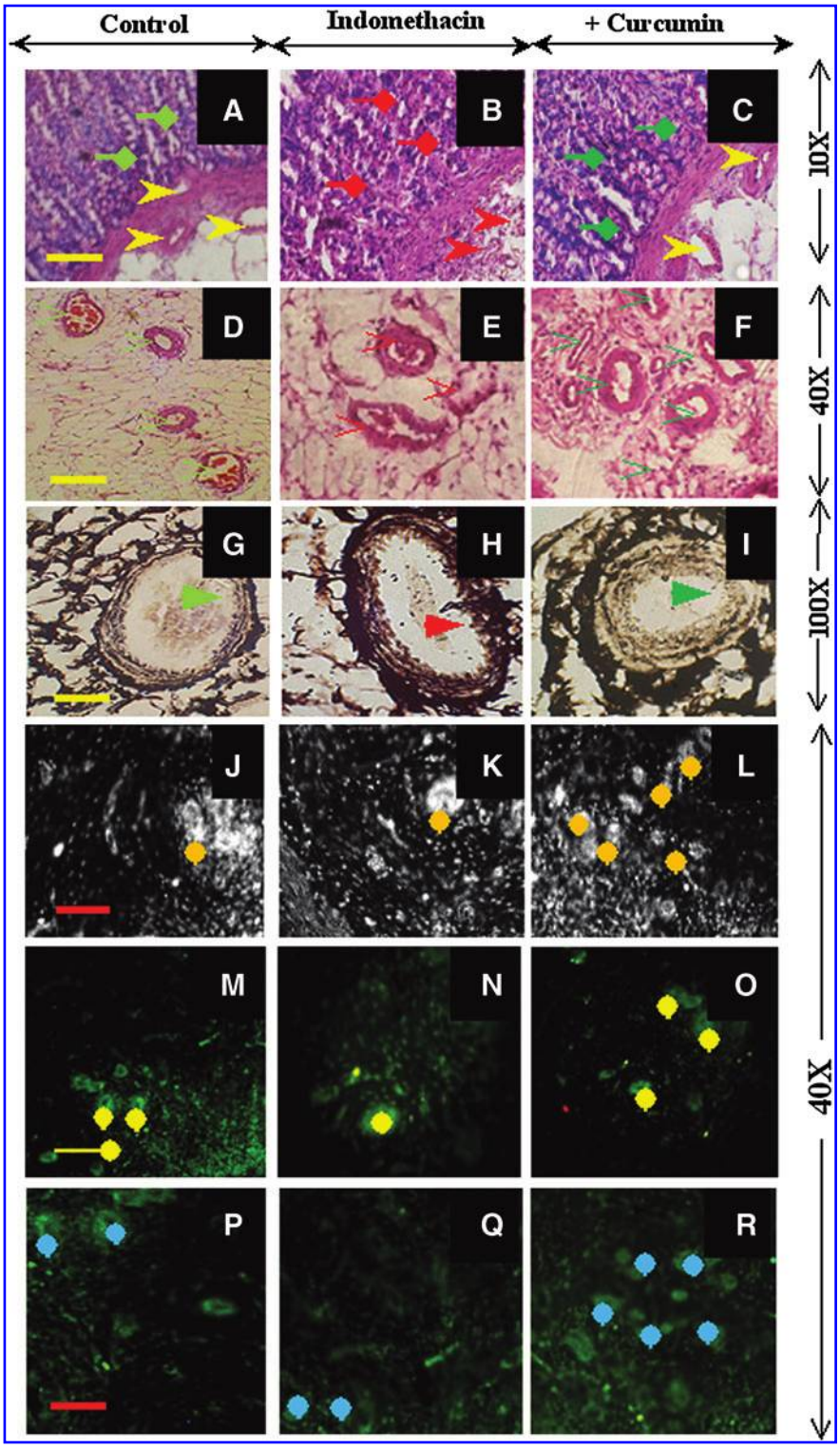

FIG. 1. Effect of curcumin on angiogenesis following ulceration in rat gastric tissues. Gastric ulcer was induced in rats by oral administration of indomethacin (48 mg/kg b.w.) and curcumin (60 mg/kg b.w.) was administered i.p. prior to indomethacin treatment. Control rats received vehicle only. After 4 h, rats were sacrificed and stomachs were processed for histological analysis as described in "Materials and Method". The histological appearance of gastric mucosa and submucosal blood vessels, stained with H&E and silver nitrate. Histological images of mucosa and submucosa in **(A)** control **(B)** indomethacin treated/ulcerated and **(C)** curcumin pre-treated indomethacin treated tissues at 10X magnification. Histological images of blood vessels in submucosa in **(D)** control **(E)** indomethacin treated/ ulcerated and **(F)** curcumin pre-treated indomethacin treated tissues at 40X magnification. Histological images shows structural detail of silver stained submucosal blood vessels in **(G)** control **(H)** indomethacin treated/ ulcerated and **(I)** curcumin pre-treated indomethacin treated tissues at 40X magnification. Gastric mucosal cells are shown by diamond arrows, blood vessels of submucosa by stealth arrows, disrupted blood vessels by open arrows and detailed structure of blood vessel by arrows respectively. Color of all arrows are demarcated as control by light green, Indomethacin by red and +curcumin by green respectively. Phase contrast images of **(J)** control, **(K)** indomethacin treated/ ulcerated and **(L)** curcumin pretreated indomethacin treated gastric tissues. Blood vessels are shown by upright orange oval arrow. Immunostaining of VEGF on endothelial cells shown by upright yellow oval arrows in **(M)** control, **(N)** indomethacin treated/ ulcerated, and **(O)** curcumin pre-treated indomethacin treated gastric tissues. MMP-2 immunostaining of endothelial cells shown by upright blue oval arrows in **(P)** control, **(Q)** indomethacin treated/ ulcerated, and **(R)** curcumin pre-treated indomethacin treated gastric tissues. Bars represent 25 μm in each panel (A-R) respectively. (To see this illustration in color the reader is referred to the Web version of this article at www.liebertonline.com/ars).

Role of regulatory molecules in reduction of MMP-2 activity during ulceration and the effect of curcumin

In our previous report, we demonstrated that MMP-2 overexpression and activity is associated with accelerated angiogenesis (6). In this study, we observed an approximately 9-fold increase in MMP-2 expression during curcumin-mediated gastroprotection (Fig. 3A, B). Interestingly, MT1-MMP expression increased approximately 2-fold whereas TIMP-2 expression decreased approximately 2-fold in curcumin-pretreated tissues. Because VEGF and TGF-β are well-known angiogenic modulators, we determined their expression at both the protein and messenger ribonucleic acid (mRNA) levels. VEGF and TGF-β expression increased approximately 4-fold

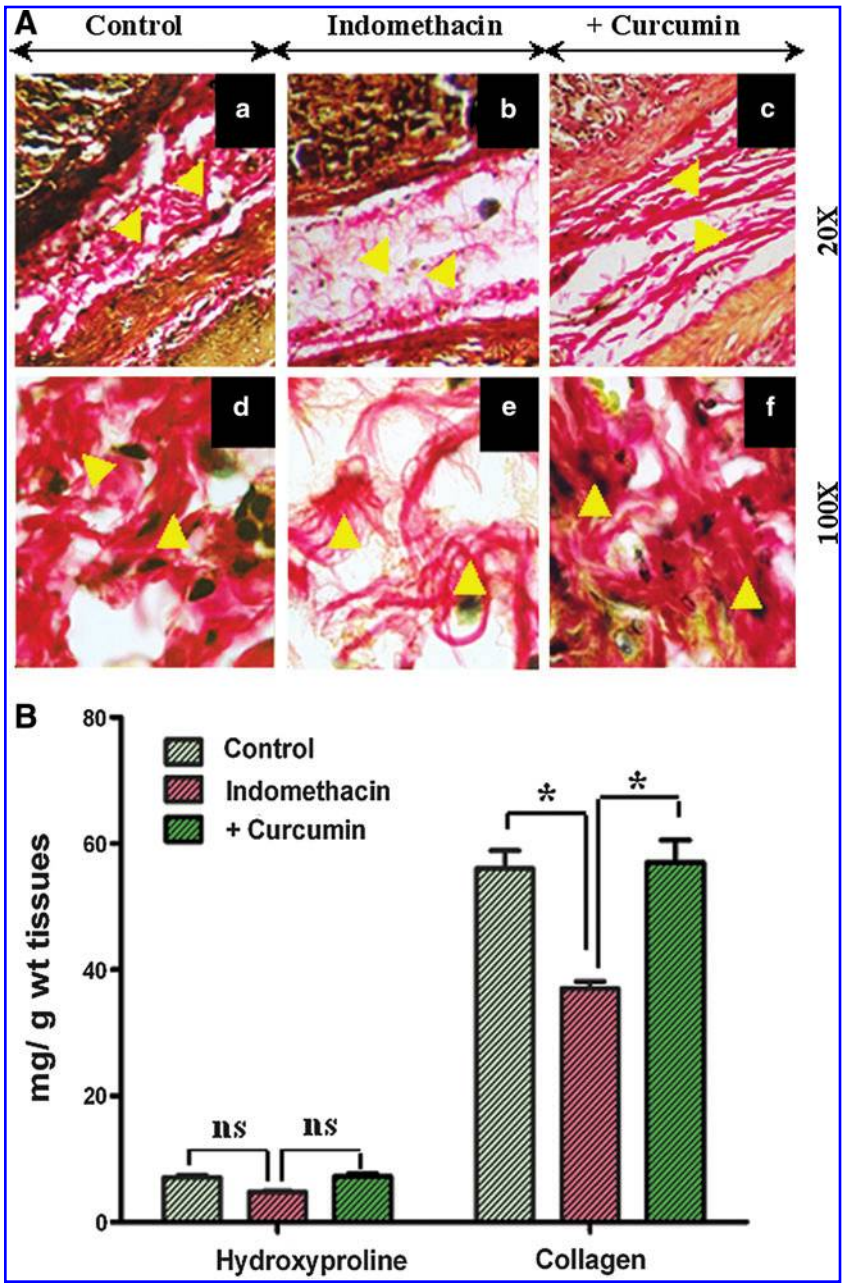

FIG. 2. Histological detection of collagen fibers in rat gastric tissues after ulceration and prevention by curcumin treatment. Stomachs from control, indomethacin treated and curcumin pretreated indomethacin treated rats were processed for histological analysis as described in "Materials and Method." **(A)** Histological appearance of collagen fibers in submucosa of **(a** and **d)** control **(b** and **e)** indomethacin treated and **(c** and **f)** curcumin pre-treated indomethacin treated tissues stained with Van Gieson's stain and observed at 20X and 100X magnification for upper and lower panel respectively. Hydroxyproline assay was done by chloramine T oxidation as described in "Materials and Methods." Measurement of hydroxyproline and collagen content in **(B)** control, indomethacin treated/ulcerated and curcumin-pretreated indomethacin treated gastric tissues as represented in histogram from four independent experiments. Densitometry values of hydroxyproline and collagen contents were compared with indomethacin treated tissues versus control tissues and curcumin pretreated indomethacin treated tissues versus indomethacin treated tissues by Bonferroni Post-tests two way ANOVA analysis by GraphPrism Instat 5 software. Error bar mean ± SEM. $p > 0.05$ NS; *, $p < 0.001$. (To see this illustration in color the reader is referred to the Web version of this article at www.liebertonline.com/ars).

each in curcumin-pretreated tissue (Fig. 3A, B). β-actin was used as a loading control (Fig. 3A). Figures 3C and 3D show that MMP-2 and MT1-MMP gene expression increased approximately 2.5-fold after curcumin pretreatment, whereas TIMP-2 expression decreased approximately 1.5-fold during gastroprotection. VEGF and TGF-β expression was inhibited during ulceration; however, curcumin reversed this effect and returned the expression to control levels and prevented wounding (Figure 3C, D). Glyceraldehyde 3-phosphate dehydrogenase (GAPDH) was used as a loading control (Fig. 3C).

Curcumin promoted angiogenesis in a chick chorioallantoic membrane model

To complement the investigation of the angiogenic potential of curcumin, we performed an angiogenic assay using a CAM model. Implantation of a curcumin-impregnated disc (80 μg) resulted in approximately 3.5- and 2.7-fold increases in the length and branching points, respectively, of blood vessels in the CAM model (Fig. 4C, D) compared to those in vehicle-impregnated vessels (Fig. 4A, D). Implantation of an indomethacin-impregnated disc in the CAM model resulted in the inhibition of angiogenesis (Fig. 4B, D). The angiogenic potential of curcumin was further substantiated by a Matrigel assay (Figure 4E). Our results strongly suggest that curcumin inhibited tube formation at increasing doses; at 200 μM, the cells were dispersed. However, at lower doses (0.2–10 μM), curcumin showed potent tubulogenesis with maximum tube formation observed at a dose of 1 μM of curcumin.

Involvement of curcumin in angiogenesis and collagenolysis—Auto healing versus curcumin-mediated healing of gastric ulceration

Rats were treated with either curcumin or vehicle following ulcer induction. Gastric tissues were processed at different

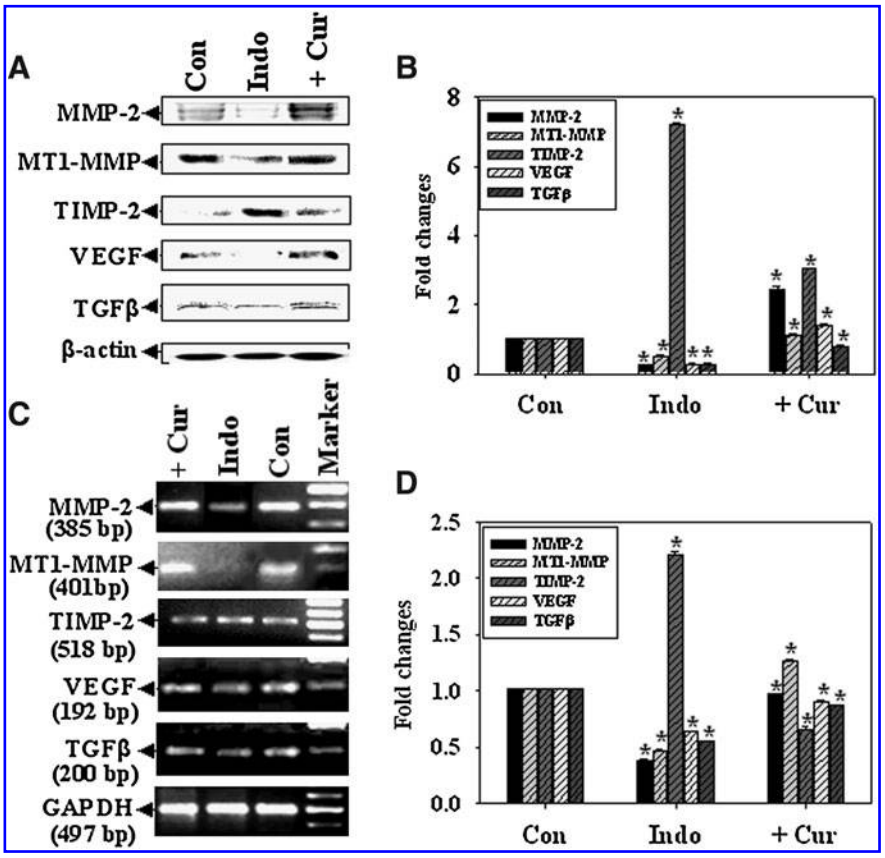

FIG. 3. Protein and messenger ribonucleic acid (mRNA) expression of regulatory molecules during prevention of gastric ulcer by curcumin. PBS extracts (120 (g) of control, ulcerated and curcumin-pretreated tissues were subjected to **(A)** Western blot and probed separately with different polyclonal antibodies: anti-MMP-2, anti-MT1-MMP, anti-TIMP-2, anti-VEGF, anti-TGFβ and anti-(-actin antibodies. Histographic representation **(B)** of fold changes in individual protein bands as measured by Lab image designed densitometry values from above blots and three other representative blots from independent experiments in each case. The densitometric data of protein bands of curcumin pretreated indomethacin treated tissues were compared with indomehacin treated tissues and indomethacin treated tissues with control tissues by Bonferroni Post-tests two way ANOVA analysis by GraphPrism Instat 5 software. Error bar mean ± SEM. *, $p < 0.001$. Using RT-PCR analysis, the expression of MMP-2, MT1-MMP, TIMP-2, VEGF, TGFβ1 and GAPDH mRNA transcripts were studied in ulcerated and healed tissues and compared with corresponding mRNA transcripts in control tissues. PCR products stained with ethidium bromide were electrophoresed in a 2% agarose gel. RT-PCR products of total RNA **(C)** derived from control, indomethacin treated and curcumin pretreated gastric tissues using specific primers for MMP-2, MT1-MMP, TIMP-2, VEGF, TGFβ1 and GAPDH representing the bands of 385, 401, 518, 192, 200 and 497 base pairs respectively. Histographic representation of fold changes in individual product **(D)** bands as measured by Lab image designed densitometry values from above blots and three other representative blots from independent experiments in each case. The data of densitometric values of PCR amplicons of curcumin pretreated indomethacin treated tissues were compared with indomethacin treated tissues and indomethacin treated tissues with control tissues by Bonferroni Post-tests two way ANOVA analysis by GraphPrism Instat 5 software. Error bar mean ± SEM. *, $p < 0.001$.

times during auto healing and curcumin-mediated healing experiments and then analyzed for cellular injury, as shown in Table 1. It is notable that curcumin accelerated healing from 8 h after ulceration and was prominent over a range of 8–24 h, whereas autohealing began 12 h after ulceration and the 24-h autohealed tissues were comparable to the 12-h curcumin-healed tissues. Cellular injury was significantly arrested, providing time for both autohealing and curcumin-mediated healing (Table 1).

Figures 5A–D show that during the early stages (0–8 h) of autohealing, blood vessels were dilated and disrupted, and thrombi persisted inside the vessels for 24 h. In contrast, disrupted blood vessels were not seen at 8 h, and at 24 h the gastric tissues had an increased number of vessels compared to that at 0 h in curcumin-treated rats, suggesting the angiogenic potential of curcumin (Fig. 5E–H). Quantitative analysis of angiogenesis is shown in Figure 5I. At 24 h, curcumin augmented vessel formation approximately 25-fold and repaired injured vessels approximately 6-fold compared to at 0 h of ulceration. Considerable differences in the density and integrity of collagen fibers were also observed in curcumin-mediated healing compared to those in autohealing. During autohealing, collagen fibers were found to be thin, sparse, and disordered from 4 h to 8 h, but there was a partial deposition of collagen fibers at 24 h (Fig. 6A–D). In contrast, during curcumin-mediated healing, the deposition of collagen fibers became evident as early as at 8 h and was intense at 24 h after ulceration (Fig. 6E–G).

Involvement of regulatory molecules during auto healing and curcumin-mediated healing

To elucidate the molecular mechanism of curcumin-mediated healing, *in vivo* time course MMP-2 expression was investigated in ulcerated and healed tissues (Fig. 7A, B). During autohealing, proMMP-2 and active MMP-2 activities were increased approximately 1.5- and 15-fold, respectively, at 24 h compared with those at 0 h after ulceration. Interestingly, active MMP-2 activity increased approximately 15-fold even at 8 h after ulceration and approximately 30-fold at 24 h after ulceration during curcumin-mediated healing (Fig. 7A, B). During autohealing, MMP-2 and MT1-MMP expression increased approximately 15- and 6-fold, respectively, at 24 h, whereas no significant expression was detected at 4 h.

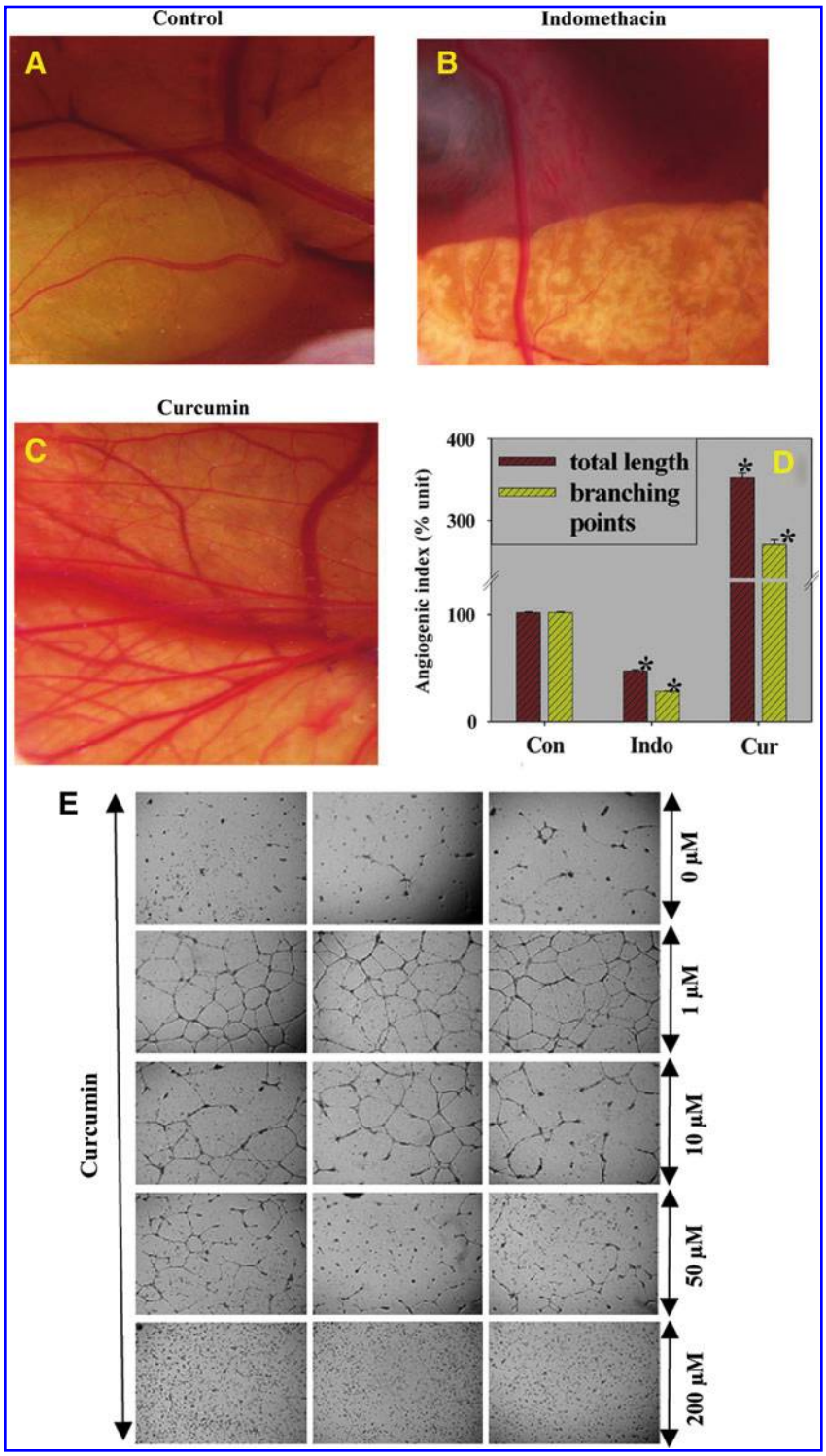

FIG. 4. Angiogenic potential of curcumin on chick chorioallantoic membrane and Matrigel assay. Carboxymethylcellulose discs impregnated with **(A)** vehicle **(B)** indomethacin and **(C)** curcumin were implanted in CAM as described in "Materials and Method." **(D)** Histographic representation of angiogenic index of control, indomethacin and curcumin implanted CAM from above experiment and three other representative experiments. The data of angiogenic index of indomethacin was compared with vehicle and those for curcumin with indomethacin by Bonferroni Post-tests two way ANOVA analysis by GraphPrism Instat 5 software. Error bar mean ± SEM. *, $p < 0.05$. **(E)** Different concentration of HUVEC cells were cultured in DMEM media to optimize the number of cells for studying angiogenic effect of curcumin. Six well culture plates were used to culture 4X 10^4 cells per well. Different doses of curcumin (1.0, 10.0, 50 and 200.0 μM concentration from top to bottom) was added in HUVEC culture media and incubated overnight at 37° C incubator. Data are represented as triplicates. (To see this illustration in color the reader is referred to the Web version of this article at www.liebertonline.com/ars).

Curcumin accelerated MMP-2 and MT1-MMP expression approximately 6-fold each at 4 h compared to that at 0 h after ulceration. TIMP-2 expression decreased significantly, even at 8 h, during curcumin-mediated healing compared to that at 24 h during autohealing (Fig. 7C, D). Because VEGF and TGF-β modulate physiological angiogenesis *via* proMMP-2 activation, we determined their expression levels in a therapeutic model of curcumin healing. VEGF expression increased approximately 4- and 16-fold 8 h after ulceration during autohealing and curcumin-mediated healing, respectively, suggesting the angiogenic potential of curcumin (Fig. 7C, D). In comparison to 0 h after ulceration, TGF-β expression was enhanced approximately 6- and 20-fold at 4 and 8 h, respectively, during autohealing, but approximately 12- and 20-fold at 4 and 8 h, respectively, during curcumin-mediated healing (Fig. 7C, D).

Table 1. Cellular Injury in Gastric Mucosa During Healing of Indomethacin-Induced Ulcer by Curcumin

Duration in hr	*Autohealing (% cell injury/inch^2)*	*Curcuminmediated healing (% cell injury/ inch^2)*	*Healing efficacy of curcumin*
0 h	58 ± 2.6	58 ± 2.6	0%
4 h	52 ± 1.7**	51 ± 0.8*	17%
8 h	36 ± 0.7*	22 ± 1.6*	64%
12 h	30 ± 1.1*	12 ± 0.5*	64%
24 h	23 ± 1.5*	4 ± 0.6*	54%
30 h	18 ± 0.6*	2 ± 0.4*	40%

Gastric ulcers were induced by indomethacin (48 mg/kg b.w.) and after 4 h, one group of rats received curcumin (60 mg/kg b.w.) while the other group received vehicle. Autohealing and curcumin-mediated healing were monitored at different time points. Rats were sacrificed at different time points and stomach tissues were processed for H&E staining. Microscopic photographs of each group at different time points were separately captured at 100X magnification under oil immersion and divided into several 1inch^2 boxes by Adobe Photoshop version 6. The injured cells in each box from mucosal areas were counted from three independent experiments of each group. Results are reported as the means ± SEM. *, $p < 0.001$; **, $p < 0.05$. The data of % cell injury of auto-healed and curcumin-mediated healed samples at different time points were compared with their respective 0 h by Bonferroni Post-tests two way ANOVA analysis by GraphPrism Instat 5 software. The healing efficacy was measured using the following formula [(value of autohealing - value of curcumin-mediated healing) ÷ (value of autohealing at 0 h - value of autohealing at respective h) × 100].

Discussion

A major finding of this study is the angiogenic effect of curcumin, which was determined using a CAM model, Matrigel assay, and rat model of gastric ulceration. Curcumin was found to restore vessel architecture by restoring the collagen matrices in ulcerated gastric tissues. The presence of curcumin inside the system before ulcer development may arrest microcirculatory damage or provide a stimulus for repair of vascular architecture, thereby preventing ulceration. Our results are in accordance with those of Fedive et al. (3) and Hasbe (9), who observed a decreased collagen content in different gastric ulcer models. Because collagen is the primary component of ECM, ulceration appears to be due to differences in ECM turnover, which are guided by the balance between deposition and degradation of collagen in gastric tissues. It is worth mentioning that angiogenesis is dependent on ECM turnover, ECM deposition, and endothelial cell proliferation (23). Khanna et al. reported that curcumin enhanced healing of cutaneous punch wounds, providing further support to our findings (17). In contrast, curcumin has also been shown to exhibit anti-angiogenic activity in fibrosarcoma cells and rabbit cornea (9, 19).

The hallmark of ulcer healing is a coordinated interplay among pro-inflammatory cytokines, growth factors, and proteases (7, 11). In the present study, VEGF and TGF-β expression decreased during ulceration, which could be explained on the basis of the unavailability of prostaglandin E_2, resulting in decreased VEGF mRNA (8). We found that curcumin hastens healing *via* a universal pro-angiogenic stimulus, namely VEGF-mediated angiogenesis and collagenization, in preventive and therapeutic models of gastric ulceration. Furthermore, suppressed TGF-β expression is associated with destruction of chief cells (13) in the ulcer milieu. TGF-β inhibits the proliferation of cultured endothelial cells, although it has a strong angiogenic effect, probably *via* VEGF biosynthesis (23) *in vivo*, which in turn promotes the synthesis of ECM components (22, 24). TGF-β expression was enhanced before VEGF expression during autohealing, and curcumin accelerated the expression of both at earlier time points in our therapeutic model. Our findings corroborate previous findings in which the addition of exogenous VEGF caused healing of gastric wounds *via* TGF-β signaling (22, 30).

Endothelial cells are known to predominantly express MMP-1, MMP-2, and MMP-9, which regulate angiogenic processes involving basement membrane degradation, ECM invasion, and cleaving cell–cell adhesion (18, 21, 23). Several studies have explained the inhibitory effect of indomethacin on angiogenesis *via* MMP-2 suppression (6, 12, 28, 29). We observed that curcumin not only overexpressed MMP-2 but also colocalized with VEGF at neovessels in healing tissues. We postulate that the overproduction of active MMP-2 is governed by VEGF signaling in healing pockets of gastric tissues. The threshold VEGF and TGF-β levels were attained at earlier time points during curcumin-mediated healing than autohealing. Moreover, curcumin stimulated tubulogenesis at low doses in the human umbilical vein endothelial cells (HUVEC) cell line. One possible explanation is that the mechanism of healing occurs *via* VEGF and MMP-2 overexpression and TIMP-1 and TIMP-2 suppression (32, 36). Other studies have postulated a universal mechanism of MMP-2 and VEGF accumulation that is governed by mucosal or chief cells and endothelial cells in gastric tissues during healing. We earlier reported that collagen type III and IV can be efficiently cleaved by activated MMP-2 *in vitro* (6). Furthermore, immunofluorescence and *in vitro* collagenase assays revealed that the availability of active MMP-2 in the gastric ECM (lamina propia) assists in the alteration of the basement membrane and vascular architecture, thereby promoting healing (6). In this study, MMP-2 upregulation occurred together with increased MT1-MMP expression but decreased TIMP-2 expression. Therefore, we postulate that MMP-2 may be activated by a MT1-MMP- and TIMP-2-dependent mechanism *in vivo* and modulate ECM homeostasis and angiogenesis during healing. TIMP-2 was also found to be downregulated at an earlier time point in curcumin-pretreated tissues, suggesting that the balance between proteases and protease inhibitors is a critical factor in the physiological setting during healing. Our preventive and healing studies together corroborate the molecular mechanism, that is, the availability of MMP-2 is indispensable in the ulcer milieu for guiding physiological angiogenesis. This is the first study to reveal that the presence of curcumin in the system before or after ulcer development may arrest microcirculatory damage or initiate neovessel formation and collagenization by recruiting VEGF and MMP-2, thereby increasing angiogenic processes during healing of gastric ulcers. In summary, we propose that curcumin as an angiogenic modulator is dependent on the pathological and physiological state of the tissue environment.

Materials and Methods

Gelatin from porcine skin, indomethacin, curcumin, Triton X-100, protease inhibitor cocktail, gelatin fused with 4% beaded agarose, Fast Blue BB salt, benzenesulfonic acid, chloramine-T and 5-bromo-4-chloro-3-indolyl phosphate/nitroblue tetrazolium solution were obtained from Sigma. Polyclonal anti-MMP-2, MT1-MMP, TIMP-2, VEGF, TGF-β, and β-actin antibodies were purchased from Santa Cruz. TRIZOL reagent, Superscript II Reverse Transcriptase, and oligo(dT) primer were purchased from Invitrogen.

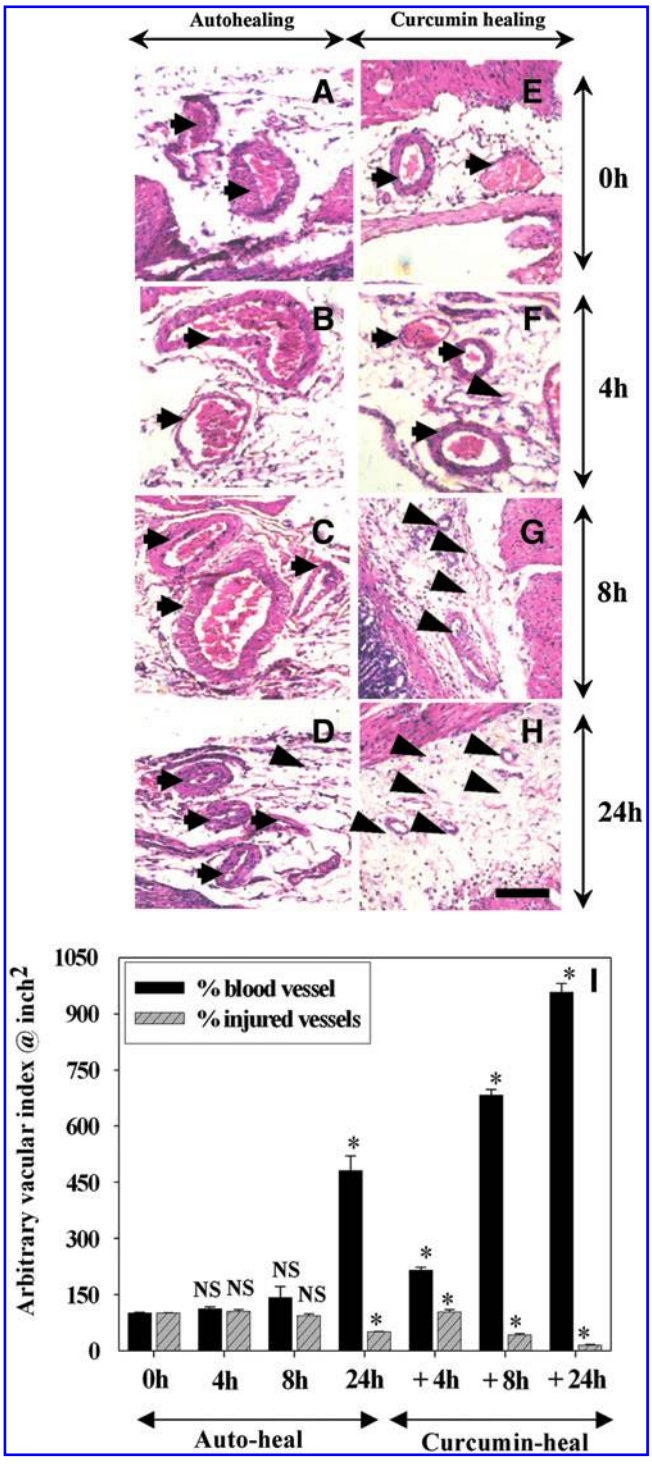

Indomethacin-induced gastric ulcer in rats—protection and healing experiments with curcumin

Animal experiments were performed following the guidelines of the animal ethics committee. Indomethacin-induced gastric ulceration developed in male Sprague-Dawley rats (180–220 g) following oral administration of 48 mg/kg bodyweight (b.w.) indomethacin. The control group received vehicle only. In some animals, 30 min before indomethacin administration, 60 mg/kg b.w curcumin was administered intraperitoneally (i.p.). The rats were then sacrificed after 4 h of indomethacin treatment, and their stomachs were collected and scored for ulcer indices (28). For healing experiments, after 4 h of indomethacin administration, one group of rats received vehicle while the other group received 60 mg/kg b.w curcumin i.p. Rats were sacrificed at different time points (i.e., 0, 4, 8, and 24 h after 4 h of indomethacin treatment) to monitor healing.

Histological studies

Gastric tissues were fixed in 10% buffered formalin and embedded in paraffin. Sections (5-μm) were stained with hemotoxylin and eosin, silver nitrate, and Van Gieson stains. For immunofluorescence experiments, antigen retrieval was performed by trypsin (0.05% trypsin, 0.1% $CaCl_2$) followed by blocking with 5% bovine serum albumin (BSA) in tris buffer saline (TBS) (20 m*M* Tris(hydroxymethyl)amino methane-HCl , pH 7.4 containing 150 mM NaCl) for 2 h. The specimens were then incubated overnight at 4°C in primary antibody solution (diluted 1:200 in TBS with 1% BSA) in a humid chamber. The sections were washed with TBS Tween 20 (TBST) and then incubated with fluorescein isothiocyanate-conjugated secondary antibody (diluted 1:400 in TBS with 1% BSA) for 2 h at room temperature and washed with TBST. Images were captured at magnifications of 20×10, 40×, and 100×10 using an Olympus microscope (1×70) and Camedia software (E-20P 5.0 Megapixel).

FIG. 5. Curcumin promotes submucosal blood vessels formation during healing of gastric ulceration. Gastric ulcers were induced by indomethacin (48mg/kg body wt). 4 h after gastric ulcers reached maximum, one group of rats received vehicle while the other group received curcumin (60 mg/ kg body wt) intraperitonially. Rats were sacrificed at different time points and stomachs were processed for H&E staining as described in "Materials and methods". Left panel shows submucosal blood vessels (40X) at **(A)** 0 **(B)** 4 **(C)** 8 and **(D)** 24h during autohealing and right panel shows at **(E)** 0 **(F)** 4 **(G)** 8 and **(H)** 24h during curcumin-mediated healing. Normal, damaged and newly formed blood vessels cells are shown by big arrow, small arrow and arrowhead respectively. Bars represent 25 μm for left and right panel **(A–H)** respectively. Histological photographs of both auto and curcumin mediated healed tissues were captured and analyzed by Adobe Photoshop program. Histographic representation of angiogenic index **(I)** of tissues at various time points as compared to 0h of maximum ulcertion from above experiment and three other representative experiments. The data of angiogenic index of autohealed and curcumin pretreated tissues were compared with 0h of maximum ulcerated tissues by Bonferroni Post-tests two way ANOVA analysis by GraphPrism Instat 5 software. Error bar mean ± SEM.*, $p < 0.001$, # $p < 0.01$. (To see this illustration in color the reader is referred to the Web version of this article at www.liebertonline.com/ars).

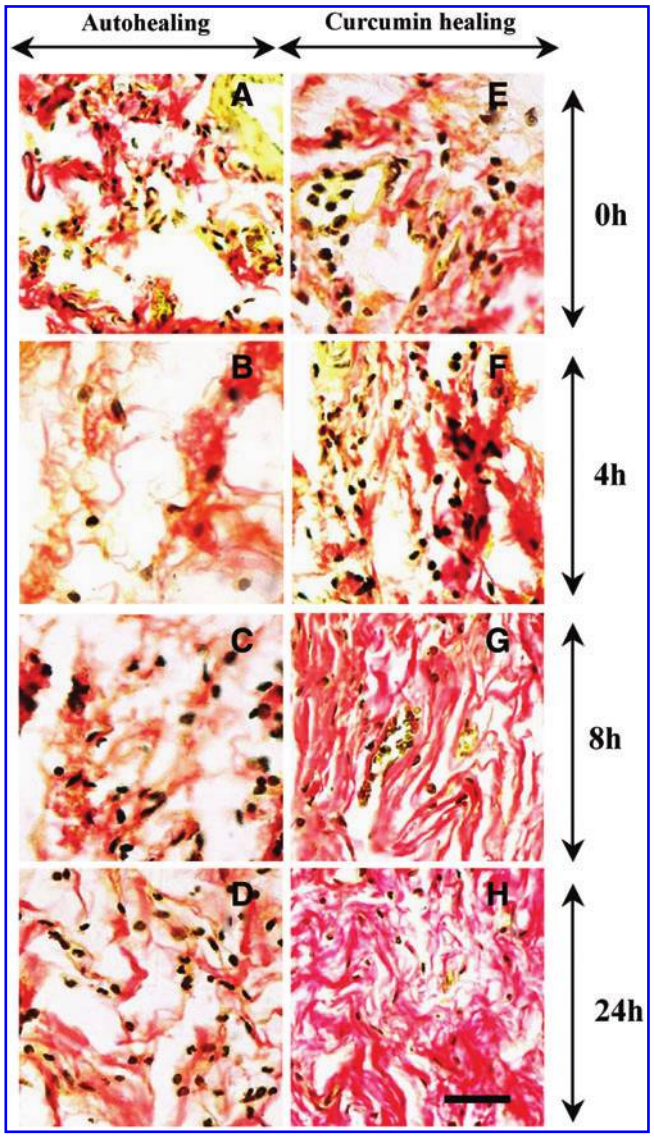

FIG. 6. Examination of collagen matrices of rat gastric tissues during autohealing and curcumin-mediated healing. Autohealing and curcumin-mediated healing experiments were done as described in Fig. 4, rat stomachs were processed for Van Gieson's stain as described in "Materials and Method". The histological appearance of submucosal collagen fibers as a function of time during autohealing and curcumin mediated healing. Left panel shows deposition of collagen fibers (40X) at **(A)** 0 **(B)** 4 **(C)** 8 and **(D)** 24 during autohealing and right panel shows deposition of collagen fibers (40X) at **(E)** 0 **(F)** 4 **(G)** 8 and **(H)** 24 h during curcumin mediated healing of ulcerated tissues. Bars represent 25 μm for left and right panel **(A–H)** respectively. (To see this illustration in color the reader is referred to the Web version of this article at www.liebertonline.com/ars).

Collagen estimation

Tissues obtained from all three groups were dried to a constant weight and hydrolyzed in 6 N HCl for 4 h at 130°C. The hydrolyzed samples were then adjusted to a pH of 7 and subjected to chloramine-T oxidation for 20 min. The colored adduct formed with Ehrlich reagent at 60°C was read at 557 nm. Hydroxyproline, which is considered a marker of collagen synthesis, was run concurrently as a standard and values were reported as mg/g dry weight of tissue (35).

Chick chorioallantoic membrane model

The angiogenic activity of curcumin was examined using the CAM model (16). Day 0 fertilized eggs of white leghorn chickens were kept at 37°C under sterile conditions. After 9 days, either indomethacin- (20 μg) or curcumin- (20, 40, and 80 μg) impregnated carboxymethylcellulose discs were implanted in the CAM models through a 1 cm^2 window made on the shells of different eggs. Control eggs were implanted with vehicle-impregnated discs in an identical manner. After resealing, eggs were incubated at 37°C in a humidified chamber for 72 h, opened, and observed macroscopically. Quantitative measurements of the branching points and length of the vessels were performed after capturing photographs and were computed using Adobe Photoshop.

Capillary tube formation by HUVEC cells in Matrigel

To examine the effect of curcumin on tubulogenesis, HUVEC cells (40,000 cells/well) were simultaneously seeded with curcumin (0.2, 1.0, 10.0, 50, and 200 μM) in 6-well culture plates precoated with Matrigel (Fisher Scientific). Tube formation was observed periodically using a phase contrast microscope. The representative Polaroid images shown in the results were taken 24 h after curcumin administration.

Quantification of the angiogenic index and inflammatory cell infiltration

Microscopic photographs of tissues in each group were separately captured at a magnification of 100× under oil immersion and divided into several 1-$inch^2$ boxes by Adobe Photoshop version 6.0. Normal, disrupted, and newly formed blood vessels as well as infiltrated inflammatory cells in each submucosal specimen were counted, with three independent experiments for each group. Data relating to the angiogenic index and cell infiltration in different tissue groups were compared with regard to the prevention of ulceration by curcumin.

Tissue extraction and gelatin zymography

Gastric tissue specimens were suspended in phosphate-buffered saline containing a protease inhibitor cocktail, minced, and then incubated for 10 min at 4°C. After centrifugation at 12,000 *g* for 15 min, the supernatant was collected and electrophoresed on 8% non-reducing SDS-polyacrylamide gels containing 1 mg/ml gelatin, under non-reducing conditions, washed with 2.5% Triton X-100, incubated in calcium assay for 18 h at 37°C and stained with 0.1% Coomassie blue before destaining (28).

Western blotting

Proteins (120 μg) were electrophoresed on 8% non-reducing SDS-polyacrylamide gels and transferred to a

nitrocellulose membrane. The membrane was blocked for 2 h with 20 m*M* TBST containing 3% BSA solution, followed by overnight incubation in 1:200 dilutions of different primary antibodies. The membrane was washed with TBST and incubated with alkaline phosphatase-conjugated secondary antibody. The bands were visualized using a 5-bromo-4-chloro-3-indolyl phosphate/nitroblue tetrazonium substrate solution.

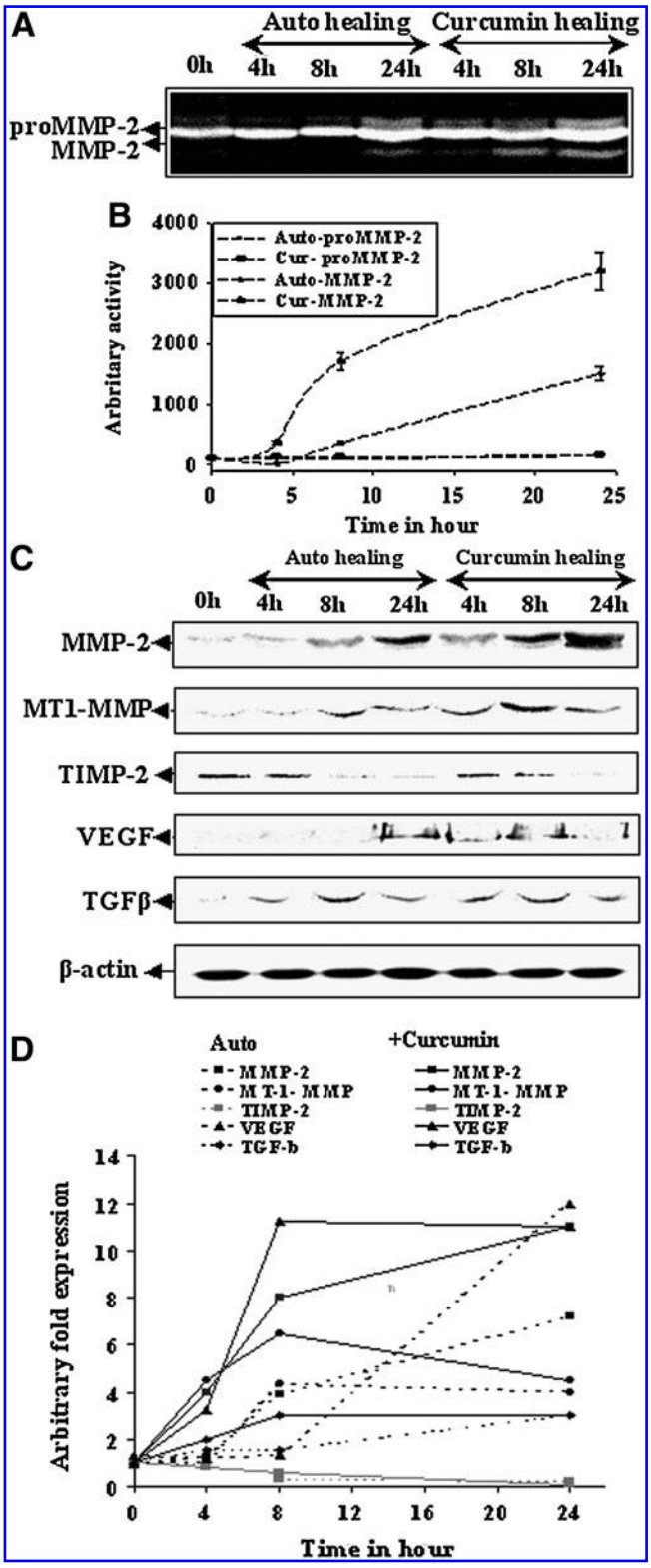

Reverse transcriptase-polymerase chain reaction

Total cellular RNA was extracted from mucosa of gastric tissues with TRIZOL reagent and quantified by measuring absorbance at 260 nm. Complementary DNA was synthesized using 1 μg of total RNA from each sample in a 20-μl reaction buffer with Superscript II reverse transcriptase and an oligo$(dT)_{15}$ primer. Complimentary DNA was amplified against forward and reverse primers of MMP-2 (5′-ATGGCTTCC TCTGGTGCT-3′ and 5′-TCGTAGTGGTTG TGGTTGC-3′), MT1-MMP (5′-ATGGCACCCTTTTACCAGTG-3′ and 5′-AA CACCCAATGCTTGTCTCC-3′), TIMP-2 (5′-AAAGCAGTGA GCGAGAAGGAGGTG-3′ and 5′-GGG TCCTCGATGTCAA GAAACTC-3′), VEGF (5′-TTGAGACCCTGGTGGACATC-3′ and 5′-CTCCTATGTGCTGGCTTTGG-3′), TGF-β1 (5′-CAACA ATTCCTGGCGTTACC-3′ and 5′-TGGGACTGATCCCATTG ATT-3′), and GAPDH (5′-TGGGGTGATGCTGGTGCTGAG-3′ and 5′-GGTTTCTCCAGGCGGCATGTC-3′). The polymerase chain reaction (PCR) reactions included 35 cycles of denaturation (94°C for 30 s), annealing (54–59.5°C for 30 s), and extension (72°C for 60 s). The PCR products were fractionated on 2% agarose gels and visualized by ethidium bromide staining.

Statistical analysis

Data were fitted using Sigma plot and are presented as mean ± SEM. Statistical analysis was performed using Bonferroni-corrected two-way analysis of variance (ANOVA) in GraphPrism Instat 5 software.

Acknowledgments

This work was supported by IAP001 from the Council of Scientific and Industrial Research, New Delhi, India. Lijun Zhan is acknowledged for her contribution in the Matrigel assay and ENAGO Crimson Interactive, India, for editing.

FIG. 7. Involvement of regulatory molecules in angiogenesis and collagenolysis during autohealing and curcumin-mediated healing. Gelatin zymography of **(A)** equal amounts of PBS extracts (80μg) from auto and curcumin healed tissues at different time points. Graphical representation **(B)** of pro- and active MMP-2 as measured by Lab Image densitometry program from the above zymogram and two other representative zymograms from independent experiments in each case. Western blot analysis **(C)** using 120 μg of protein of PBS extract from gastric tissues of auto healing and curcumin-mediated healing at different time points and probed separately with anti-MMP-2, anti-MT1-MMP, anti-TIMP-2, anti-VEGF, anti-TGFβ and anti-(-actin antibodies. Graphical representations of fold changes in **(D)** individual protein bands as measured by Lab image designed densitometry values from above blots and three other representative blots from independent experiments in each case. The data of angiogenic index of autohealed and curcumin pretreated tissues were compared with 0h of post ulceration by Bonferroni Post-tests two way ANOVA analysis by GraphPrism Instat 5 software. Error bar mean ± SEM. *, $p < 0.001$, # $p < 0.01$, NS, non-significant.

Author Disclosure Statement

No competing financial interests exist.

References

1. Dai XP, Li JB, Liu ZQ, Ding X, Huang CH, Zhou B. Effect of Jianweiyuyang granule on gastric ulcer recurrence and expression of VEGF mRNA in the healing process of gastric ulcer in rats. *World J Gastroenterol* 11: 5480–5484, 2005.
2. Dorai T, Cao Y-C, Dorai B, Buttyan R, Katz AE. Therapeutic potential of curcumin in human prostate cancer. III. Curcumin inhibits proliferation, induces apoptosis, and inhibits angiogenesis of LNCaP prostate cancer cells in vivo. *The Prostate* 47: 293–303, 2001.
3. Fediv OI, Meshyshen IF, Kolomoiets M. [Connective tissue proteins from an erosive stomach ulcer]. *Ukr Biokhim Zh* 66: 101–107, 1994.
4. Fisher C, Gilbertson-Beadling S, Powers EA, Petzold G, Poorman R, Mitchell MA. Interstitial collagenase is required for angiogenesis in vitro. *Dev Biol* 162: 499–510, 1994.
5. Fries JF, Miller SR, Spitz PW, Williams CA, Hubert HB, Bloch DA. Toward an epidemiology of gastropathy associated with nonsteroidal antiinflammatory drug use. *Gastroenterology* 96: 647–655, 1989.
6. Ganguly K, Sharma AV, Reiter RJ, Swarnakar S. Melatonin promotes angiogenesis during protection and healing of indomethacin-induced gastric ulcer: role of matrix metaloproteinase-2. *J Pineal Res* 49: 130–140, 2010.
7. Gardiner TA, Gibson DS, de Gooyer TE, de la Cruz VF, McDonald DM, Stitt AW. Inhibition of tumor necrosis factor-alpha improves physiological angiogenesis and reduces pathological neovascularization in ischemic retinopathy. *Am J Pathol* 166: 637–644, 2005.
8. Ghosh AK. Regulation by prostaglandin E2 and histamine of angiogenesis in inflammatory granulation tissue. *Yakugaku Zasshi* 123: 295–303, 2003.
9. Hahm ER, Gho YS, Park S, Park C, Kim KW, Yang CH. Synthetic curcumin analogs inhibit activator protein-1 transcription and tumor-induced angiogenesis. *Biochem Biophys Res Commun* 321: 337–344, 2004.
10. Hasebe T. Collagen and collagenase in ulcer tissue–2. Restraint and water immersion induced gastric lesions and effects of cimetidine and misoprostol. *Tokai J Exp Clin Med* 12: 181–190, 1987.
11. Jones MK, Tomikawa M, Mohajer B, Tarnawski AS. Gastrointestinal mucosal regeneration: role of growth factors. *Front Biosci* 4: D303–309, 1999.
12. Jones MK, Wang H, Peskar BM, Levin E, Itani RM, Sarfeh IJ, Tarnawski AS. Inhibition of angiogenesis by nonsteroidal anti-inflammatory drugs: insight into mechanisms and implications for cancer growth and ulcer healing. *Nat Med* 5: 1418–1423, 1999.
13. Kai T, Taketazu F, Kawakami M, Shimanuki K, Yamada S, Miyazono K, Kato M, Miyata M. Distribution of transforming growth factor-beta and its receptors in gastric carcinoma tissue. *Jpn J Cancer Res* 87: 296–304, 1996.
14. Khanna S, Venojarvi M, Roy S, Sharma N, Trikha P, Bagchi D, Bagchi M, Sen CK. Dermal wound healing properties of redox-active grape seed proanthocyanidins. *Free Radic Biol Med* 33: 1089–1096, 2002.
15. Lempinen M, Inkinen K, Wolff H, Ahonen J. Matrix metalloproteinases 2 and 9 in indomethacin-induced rat gastric ulcer. *Eur Surg Res* 32: 169–176, 2000.
16. Lobb RR, Alderman EM, Fett JW. Induction of angiogenesis by bovine brain derived class 1 heparin-binding growth factor. *Biochemistry* 24: 4969–4973, 1985.
17. Maheshwari RK, Singh AK, Gaddipati J, Srimal RC. Multiple biological activities of curcumin: a short review. *Life Sci* 78: 2081–2087, 2006.
18. Matrisian LM. Metalloproteinases and their inhibitors in matrix remodeling. *Trends Genet.* 6: 121–125, 1990.
19. Mohan R, Sivak J, Ashton P, Russo LA, Pham BQ, Kasahara N, Raizman MB, Fini ME. Curcuminoids inhibit the angiogenic response stimulated by fibroblast growth factor-2, including expression of matrix metalloproteinase gelatinase B. *J Biol Chem* 275: 10405–10412, 2000.
20. Papetti M, Herman IM. Mechanisms of normal and tumor-derived angiogenesis. *Am J Physiol Cell Physiol* 282: C947–C970, 2002.
21. Pepper MS. Role of the matrix metalloproteinase and plasminogen activator-plasmin systems in angiogenesis. *Arterioscler Thromb Vasc Biol* 21: 1104–1117, 2001.
22. Pertovaara L, Kaipainen A, Mustonen T, Orpana A, Ferrara N, Saksela O, Alitalo K. Vascular endothelial growth factor is induced in response to transforming growth factor-beta in fibroblastic and epithelial cells. *J Biol Chem* 269: 6271–6274, 1994.
23. Rundhaug JE. Matrix metalloproteinases, angiogenesis, and cancer: commentary re: A. C. Lockhart *et al.*, Reduction of wound angiogenesis in patients treated with BMS-275291, a broad spectrum matrix metalloproteinase inhibitor. *Clin Cancer Res* 9: 551–554, 2003.
24. Sanchez-Elsner T, Botella LM, Velasco B, Corbi A, Attisano L, Bernabeu C. Synergistic cooperation between hypoxia and transforming growth factor-beta pathways on human vascular endothelial growth factor gene expression. *J Biol Chem* 276: 38527–38535, 2001.
25. Shahin M, Gillessen A, Pohle T, Weber C, Schuppan D, Herbst H, Domschke W. Gastric ulcer healing in the rat: kinetics and localisation of de novo procollagen synthesis. *Gut* 41: 187–194, 1997.
26. Shukla A, Rasik AM, Dhawan BN. Asiaticoside-induced elevation of antioxidant levels in healing wounds. *Phytother Res* 13: 50–54, 1999.
27. Stetler-Stevenson WG. Matrix metalloproteinases in angiogenesis: a moving target for therapeutic intervention. *J Clin Invest* 103: 1237–1241, 1999.
28. Swarnakar S, Ganguly K, Kundu P, Banerjee A, Maity P, Sharma AV. Curcumin regulates expression and activity of matrix metalloproteinases 9 and 2 during prevention and healing of indomethacin-induced gastric ulcer. *J Biol Chem* 280: 9409–9415, 2005.
29. Tarnawski A, Szabo IL, Husain SS, Soreghan B. Regeneration of gastric mucosa during ulcer healing is triggered by growth factors and signal transduction pathways. *J Physiol Paris* 95: 337–344, 2001.
30. Tarnawski AS. Cellular and molecular mechanisms of gastrointestinal ulcer healing. *Dig Dis Sci* 50 Suppl 1: S24–S33, 2005.
31. Unemori EN, Bouhana KS, Werb Z. Vectorial secretion of extracellular matrix proteins, matrix-degrading proteinases, and tissue inhibitor of metalloproteinases by endothelial cells. *J Biol Chem* 265: 445–451, 1990.
32. Unemori EN, Ferrara N, Bauer EA, Amento EP. Vascular endothelial growth factor induces interstitial collagenase expression in human endothelial cells. *J Cell Physiol* 153: 557–562, 1992.
33. Wang S, Zheng Z, Weng Y, Yu Y, Zhang D, Fan W, Dai R, Hu Z. Angiogenesis and anti-angiogenesis activity of Chinese medicinal herbal extracts. *Life Sci* 74: 2467–2478, 2004.

34. White JF, Werkmeister JA, Darby IA, Bisucci T, Birk DE, Ramshaw JA. Collagen fibril formation in a wound healing model. *J Struct Biol* 137: 23–30, 2002.
35. Woessner JF, Jr. The determination of hydroxyproline in tissue and protein samples containing small proportions of this imino acid. *Arch Biochem Biophys* 93: 440–447, 1961.
36. Zucker S, Mirza H, Conner CE, Lorenz AF, Drews MH, Bahou WF, Jesty J. Vascular endothelial growth factor induces tissue factor and matrix metalloproteinase production in endothelial cells: conversion of prothrombin to thrombin results in progelatinase A activation and cell proliferation. *Int J Cancer* 75: 780–786, 1998.

Address correspondence to:
Dr. Snehasikta Swarnakar
Department of Physiology
Indian Institute of Chemical Biology
4, Raja S.C. Mullick Road
Jadavpur, Kolkata-700032
India

E-mail: snehasiktas@hotmail.com

Date of first submission to ARS Central, August 12, 2011; date of final revised submission, September 23, 2011; date of acceptance, September 25, 2011.

Abbreviations Used

BSA = bovine serum albumin
b.w. = bodyweight
CAM = chorioallantoic membrane
ECM = extracellular matrix
GAPDH = glyceraldehyde 3-phosphate dehydrogenase
HUVEC = human umbilical vein endothelial cell
i.p. = intraperitoneally
MMP = matrix metalloproteinase
mRNA = messenger ribonucleic acid
MT = membrane type
PGE_2 = prostaglandin E_2
TBS = Tris buffer saline
TGF = transforming growth factor
TIMP = tissue inhibitor of metalloproteinase
VEGF = vascular endothelial growth factor